Role of Conformational Relaxation on the Voltammetric Behavior of Polypyrrole. Experiments and Mathematical Model

ARTICLE *in* THE JOURNAL OF PHYSICAL CHEMISTRY B · OCTOBER 1997

Impact Factor: 3.3 · DOI: 10.1021/jp9714633

Role of Conformational Relaxation on the Voltammetric Behavior of Polypyrrole. Experiments and Mathematical Model

T. F. Otero,* H. Grande, and J. Rodríguez

Laboratorio de Electroquímica, Facultad de Química, Universidad del País Vasco, P.O. Box 1072, 20080 San Sebastián, Spain

Received: April 30, 1997[⊗]

Anomalous effects associated with the electrochemical cycling of electrogenerated polypyrrole films after polarization at high cathodic potentials were simulated from a derivation of the electrochemically stimulated conformational relaxation model. The cathodic treatment promotes the compaction of the polymer by conformational movements of polymeric segments. The compacted structure requires, at constant temperature, an anodic overpotential (that is, an extra energy) to be opened during oxidation, allowing the penetration of counterions from the solution in order to keep the electroneutrality in the film. The definition of a conformational relaxation time for the swelling of the polymeric structure, including both thermal and electrochemical energetic contributions, allows the integration of structural parameters on electrochemical equations. Theoretical voltammograms reproduce the effect of the different variables (cathodic potential, sweep rate, and temperature) and fit experimental results for polypyrrole films.

1. Introduction

A variety of theoretical treatments have been proposed in the last years in an attempt to explain the electrochemical switching behavior of electronically conducting polymers, such as polypyrrole or polyaniline.[1−17] In all cases a single electrochemical process (either electron transfer, counterion diffusion, or capacitive effects) is assumed to be the controlling step of the oxidation or reduction rate, independent of the chemical and physical nature of the polymer. For this reason, the validity of those models is restricted to simple electrochemical behaviors. In previous papers,[18−21] the authors presented a new theoretical model able to simulate chronoamperograms of polypyrrole that was previously submitted to high cathodic potentials for long periods of time in a variety of electrochemical conditions.[21,22] The so-called electrochemically stimulated conformational relaxation (ESCR) model takes into account that conducting polymers undergo swelling or shrinking processes as the electric potential applied to the polymer is changed to a new value.[23] This fact has been proved by the construction of electrochemomechanical devices, such as artificial muscles or actuators, where changes of volume linked to redox reactions are transformed into angular movements of more than 180°.[24−26] Moreover, experiences with smart membranes constructed from conducting polymer layers prove that the permeability of those materials toward counterions of different diameters can be varied by changing the membrane potential.[27−30] All those facts can be considered as direct evidence for the occurrence of conformational rearrangements in the solid matrix,[31−33] promoting strong structural changes which must be reflected in the electrochemical responses. In this context, the merit of the ESCR treatment was to integrate both electrochemistry and polymer science in an attempt to explain the anomalous effects observed in polypyrrole chronoamperometry.

The key idea in the ESCR model is that polypyrrole attains a compact structure under cathodic polarization. Furthermore, more cathodic potentials applied during reduction promote a higher compactness of the polymeric structure, making difficult the exchange of counterions between the polymer and the surrounding electrolytic solution during further oxidation, which therefore must be preceded by the swelling (or relaxation) of the polymeric structure. Once the amount of created free volume is enough to allow the movement of ions and solvent molecules throughout the film, oxidation is completed under counterion diffusion control. Swelling goes on during the diffusion-controlled oxidation, but conformational movements are not more rate controlling. The overall process can be understood as a transition from a 2D (only the external surface is electrochemically active) to a 3D (every polymeric chain actuates as an electrodic active interface) electrodic behavior.[34] Those structural changes are quite similar to those occurring in biological membranes and other natural devices.[35,36] For this reason, the clarification of the electrochemical processes that lead to structural transitions in conducting polymers will be enlightening for our comprehension about the mechanism of actuation of biological structures.

The ESCR treatment is an open model which can be expanded in order to include features related to amorphous polymers or applied to explain other anomalous effects in electrochemical behaviors. In this sense, the aim of this work is to extend the ECSR treatment to anodic voltammograms, providing a way to simulate voltammetric curves and to explain the delay observed in the beginning of the oxidation when the polymer is previously polarized at high cathodic potentials for long periods of time.[2,22,37,38] This was reported as a memory effect by Villeret and Nechtschein[39] and partially quantified by Odin.[37,38] Other authors referred to it as the first scan effect[40,41] or as a logarithmic relaxation.[42] The existence of those anomalous effects suggest that, under strong cathodic prepolarization conditions, oxidation kinetics in conducting polymers becomes driven by the rate at which structural changes in the solid matrix occur.

2. Experimental Details

Polypyrrole films (around 0.1 μm of thickness) were electrogenerated on a 1 cm^2 platinum sheet using an acetonitrile + 2% water mixture as solvent, 0.1 M $LiClO_4$ as electrolyte and 0.1 M pyrrole as monomer, by passing 50 mC through the

* Corresponding author. Fax: 34-43-21 22 36. E-mail: qppfeott@sq.ehu.es.
⊗ Abstract published in *Advance ACS Abstracts,* September 15, 1997.

S1089-5647(97)01463-6 CCC: $14.00

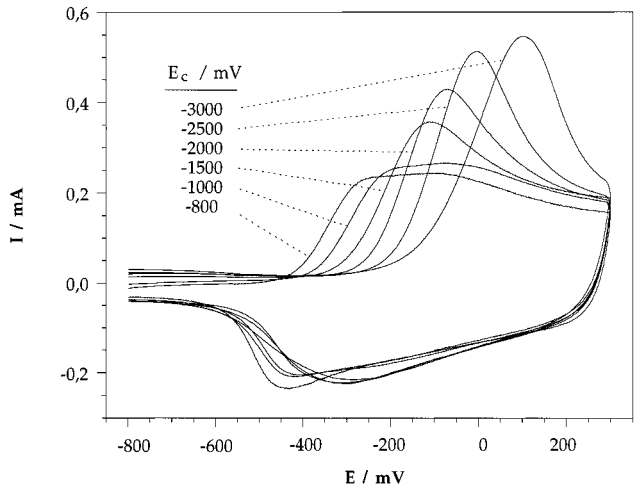

Figure 1. Experimental anodic voltammograms for thin films of polypyrrole performed in 0.1M $LiClO_4$/propylene carbonate solutions. The potential sweep was carried out between different cathodic potentials (indicated on the figure) and 300 mV vs SCE, with the scan rate of 30 mV s^{-1} and the temperature of 25 °C.

system and keeping the working electrode at 800 mV vs SCE at room temperature (25 °C). Chemicals and equipment used for synthesis are the same as in a previous work.[21] After polymerization, films were dried in air and controlled by potential sweeps in a 0.1M $LiClO_4$ solution in propylene carbonate (which was chosen as solvent because of its wide potential window). The temperature of the cell was maintained at the chosen value by means of a Huber ministat.

3. Experimental Results and Discussion

According to the ESCR model, polarization of polypyrrole films at high cathodic potentials leads not only to the reduction of the polymer but also to the compaction of the polymeric structure, thus promoting further oxidation to be controlled by conformational relaxation processes. This fact can be well studied when a polypyrrole film synthesized as described above is submitted to potential sweeps from different cathodic potentials (ranging between −3000 and −800 mV vs the saturated calomel electrode (SCE)), which are maintained for 2 min every time, until a constant anodic potential (300 mV vs SCE) is achieved at 30 mV s^{-1} and at room temperature (25 °C). Results are depicted in Figure 1. All the information related to the oxidation process can be extracted from the anodic current flowing through the external circuit along the potential sweep. When the film is prepolarized at a less cathodic potential than −800 mV vs SCE, the neutral state is attained after a few seconds of polarization and, during the subsequent anodic sweep, the beginning of the oxidation always occurs at −550 mV and the current maximum is reached at −200 mV. At higher potentials the current drops because the oxidation of the polymer is being completed. When the potential of departure is displaced to more cathodic values, oxidation initiates at more anodic potentials and the current of the maximum increases and shifts anodically. A similar effect is observed when increasing times of prepolarization at a given cathodic potential are studied.[22]

From those results it can be deduced that the cathodic potential of prepolarization controls both the oxidation potential and the oxidation rate. This can be considered as a memory effect: the position of the oxidation peak on the voltammogram indicates the cathodic potential to which the polymer was previously submitted. Otherwise, despite small variations on the position of the cathodic peaks (see Figure 1), reduction charges are quite similar, being completed at −700 mV around 90% of the reduction process. Moreover, a small reduction current (about 25 μA cm^{-2}) remains even at −3000 mV.[21] We believe that this residual reduction current is responsible for the increasing closure of the structure attained at increasing cathodic potentials. The charge consumed during oxidation is always the same regardless of the initial potential because it is only controlled by the anodic limit of potential, thus being independent of whether oxidation occurred under conformational relaxation control or by diffusion control.

Those experimental results are related, according to the ESCR interpretation, to changes in the conformations of the polymeric chains induced by an electrochemical reaction. During oxidation, electrons are extracted from the polymeric chains. As the population of polarons and bipolarons increases, attractive van der Waals interactions between neutral chains are transformed to increasing electrostatic repulsions between positive charges on neighboring chains. At the same time, electronic rearrangements along polymeric chains cause changes from single to double bonds between consecutive pyrrole units. Those two facts promote conformational changes (i.e. variations in torsional angles between consecutive pyrrole units) and lead to an increase in the interchain free volume, which is immediately occupied by counterions and solvent molecules. It must be remarked that every polymeric chain is involved in the oxidation process, thus oxidized polypyrrole can be considered to behave as a three-dimensional electrode.

When the polymer is again reduced to the neutral state, counterions are expelled to the solution and attractive van der Waals forces between neutral chains prevail. Reverse conformational changes result in a progressive shrinking of the polymer network, which leads to a decrease in the capability of counterions to move between chains.[30] Finally, at potentials lower than about −900 mV, the ionic permeability of the film falls to a value close to zero, hence counterions become trapped within the chain entanglement. As is deduced from anodic overpotentials required to open, via conformational changes, the closed structure thus allowing the entrance of counterions, the structure of the polymer film becomes more compact when the reduction potential is displaced to more cathodic values. This increasing closure seems to be related to the small cathodic current remaining on the voltammogram beyond −900 mV, and can be visualized as an electroosmotic process. The residual counterions trapped in the polymer before the reduction is completed need higher electric fields or longer times to be expelled toward the solution. They push the last solvent molecules remaining in the film and generate free volume which is occupied by the polymer segments, hence the polymer becomes compact. Higher cathodic potentials or longer polarization times lead to a more effective release of counterions and solvent molecules from the film, thus promoting a more compact structure and the formation of a 2D interface between the neutral polymer and the solution.

Subsequent oxidation involves the opening of this closed network, with formation of channels large enough to allow the penetration of counterions. This involves a transition from a 2D to a 3D electrode, and it is only possible if extra energy is supplied to the polymeric chains in order to undergo conformational changes. In an electrochemical system, working at constant temperature, the only way to get this energy is by means of an electric field. Thus, increasing anodic overpotentials are required to initiate, by means of a potential sweep, the opening of polymeric structures compacted at more cathodic potentials. If the negative limit is less cathodic than about −900 mV, the rate of further oxidation becomes limited by charge transfer or counterion diffusion through the film. Resulting voltammograms can be theoretically simulated without any consideration of conformational movements or structural modi-

fications, because those rearrangements, being always present during the oxidation, are not rate limiting under those conditions.

A second consequence of reduction at high cathodic potentials is that the oxidation process becomes nonuniform: conductive zones nucleate in well-defined points (always the same) on the polymer/electrolyte interface where the polymer entanglement is not so compact. Those irregularities are zones where interchain interactions are less intense, hence cooperative free movements of chains become possible, favoring the penetration of counterions. From those points the oxidized phase grows toward the metal/polymer interface, following the electric field across the neutral polymer whose low electric conductivity is sufficient to allow current flow. When a column of oxidized polymer is formed, it expands parallel to the metal surface. The nucleation of oxidized regions (an amorphous phase) within the reduced polymer (another amorphous phase) can be well followed on electrochromic polypyrrole films, like those studied in this work: blue circles of oxidized polypyrrole are formed and expand on a pale yellow reduced film. The average number of oxidation nuclei 5−9 per cm^2, which can be obtained from pictures of the electrode.[21] The rate of expansion of the oxidized regions depends on both the compactness of the polymer, which is controlled by the cathodic potential of departure, and the amount of free energy available by polymeric chains to move between different conformations, which can be supplied through the applied potential, resulting in an increase of the expansion rate all along the anodic sweep until coalescence of the growing regions.

Another way to supply the energy required for conformational movements is by means of changes in the temperature of the system. To study the influence of temperature in the conformational relaxation process, a polypyrrole film was compacted under a cathodic potential of −2000 mV (a conformational relaxation control of further oxidation is hence guaranteed) for 2 min at room temperature. The electrode was then extracted from the solution and maintained in a nitrogen flow while the solution was thermostated to a value ranging between −10 and 40 °C. Once a constant temperature was attained, the electrode was again immersed in the solution and immediately submitted to a potential sweep between −2500 and 300 mV vs SCE at 30 mV s^{-1}. The same procedure was repeated each time, compacting the film at room temperature and performing the voltammogram at the chosen temperature. Anodic branches of the voltammograms are represented by Figure 2. As the cathodic polarization is performed every time under the same experimental conditions, no differences in the degree of compactness attained along reduction at the beginning of the potential sweep exist. Therefore, any variation in the voltammogram must be due to thermal effects on the conformational relaxation rate. As predicted by the ESCR model, the nucleation occurs at the same potential each time because it is a function of the attained compactness. Once the oxidation process is initiated, current intensities increase with temperature during the anodic scan, i.e. higher energies are available by consecutive pyrrole units to undergo bond rotations. At low temperatures (see the curve corresponding to −10 °C), the relaxation rate was so slow that oxidation was not completed once the anodic limit was reached.

Conformational relaxation processes consume not only energy but also time. Thus, another variation in the rate of the opening process will arise from changing the potential sweep rate in voltammograms performed between −2000 and 300 mV at room temperature (see Figure 3). If the voltammogram is performed at a low sweep rate (for instance, 1 mV s^{-1}), conformational changes have enough time to occur, and a sharp anodic peak will appear very close to the beginning of the oxidation. When the sweep rate is increased (until 50 mV s^{-1}), shorter times are

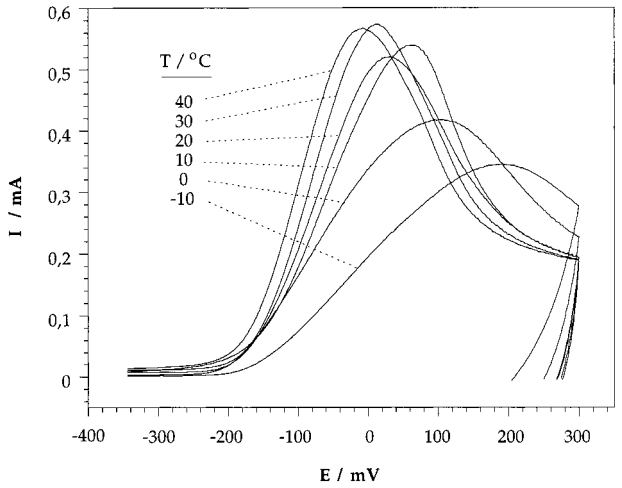

Figure 2. Experimental responses to anodic potential sweeps carried out on a polypyrrole electrode in a 0.1M $LiClO_4$/propylene carbonate solution from −2000 to 300 mV, at 30 mV s^{-1} and different temperatures ranging between −10 and 30 °C. Cathodic prepolarization was always performed at 25 °C, and it was maintained for 2 min, avoiding any difference in the degree of closure of the polymeric entanglement at the beginning of the potential sweep.

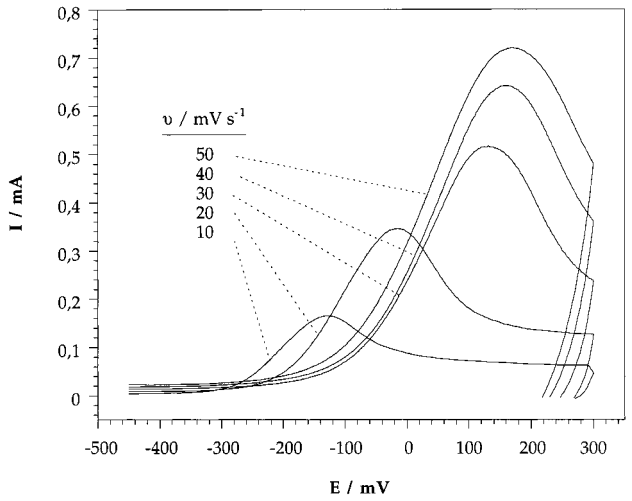

Figure 3. Experimental voltammograms obtained for thin films of polypyrrole in 0.1M $LiClO_4$/propylene carbonate solutions. The potential sweep was carried out between −2000 and 300 mV vs SCE at 25 °C, and the sweep rate was varied from 10 to 50 mV s^{-1}. The figure shows the observed evolution of the current current peak with scan rate. A linear plot is obtained, in good agreement with experimental results for thin polypyrrole films.

available to cross over the same potential after nucleation and hence, under constant compaction conditions, the rate of expansion of the oxidized regions will be lower. Thus lower currents are expected, as observed in Figure 3, whereas the current peak rises and shifts anodically.

4. Theoretical Section

The electrochemical switching of polypyrrole between its reduced and oxidized states involves various steps such as charge transfer, counterion diffusion, and conformational rearrangement. After being cathodically prepolarized however, oxidation becomes controlled by conformational relaxation processes, as is clear from experimental results. Our theoretical approach is thus focused from a structural point of view. We have divided the oxidation reaction under conformational relaxation control into three parts. An initial nucleation-like process takes place when the electric potential reaches an adequate value. The difference between this potential (E_N) and the potential for the

beginning of the oxidation in absence of any cathodic prepolarization (E_o) can be considered as a nucleation overpotential (η_N). This process is followed by the expansion of the oxidized regions at the expense of the neutral polymer, with the growth rate being controlled by a physical process of structural relaxation on the borders of the conducting zones. The electric charge spent during this process will be named relaxation charge (Q_r). Once the structure is partially open, counterions can move easier across the polymer. Therefore, the oxidation of the relaxed segments is already completed under kinetic control of the diffusion of counterions toward the oxidation centers on the polymeric chains.[43] This process consumes the diffusion charge (Q_d). Once the coalescence between conductive zones takes place, diffusion becomes the controlling step of the oxidation kinetics. Starting from a reduced but open structure (that is, not compacted by a previous cathodic treatment), all the oxidation will occur under diffusion control, with the process being initiated at lower anodic potentials. In general, the overall oxidation process will be described as an overlap of nucleation, conformational relaxation, and diffusion processes taking place in the solid state.

A mathematical definition of these processes is provided below and is similar to that deduced from chronoamperograms.[18−21] A simple nucleation model is deduced from kinetic considerations about the structure closure process taking place during the cathodic prepolarization. The radial growth rate of the cylinders formed from the oxidation nucleus can be deduced from the classical Arrhenius equation for the conformational relaxation time, depending on a conformational enthalpy that is the sum of the electrochemical and structural terms, together with an Avrami's treatment for the coalescence between conducting zones at high potentials. Finally, a simplified form of Fick's law is applied to obtain the current consumed during the diffusion-controlled oxidation. An overall equation for the electrochemical oxidation of polypyrrole films is then obtained.

Relaxation Time. The first step in the development of an electrochemical model of polymeric relaxation involves the definition of the conformational relaxation time (τ) as the average time required to change the conformation of a polymeric segment (here considered as the minimum chain length of which conformational changes allow the penetration and expulsion of ions and solvent molecules) that is reduced at a cathodic potential E_c when submitted to an anodic potential E, which is variable along the potential scan. This relaxation time is related to the energy required to complete the conformational rearrangements of a mol of polymeric segments (ΔH), in the form of an Arrhenius law:

$$\tau = \tau_o \exp[\Delta H/RT] \tag{1}$$

The energy necessary for each individual process of relaxation can be expressed as the sum of three terms:

$$\Delta H = \Delta H^* + \Delta H_c - \Delta H_e \tag{2}$$

ΔH^* is the conformational energy consumed per mol of polymeric segments in the absence of any external electric field. ΔH_c is the increase in conformational energy due to the closure of the polymer matrix during cathodic polarization. In a first approximation, ΔH_c is assumed to be proportional to the cathodic overpotential (η_c), which is related to the potential of closure of the polymer structure during a cathodic potential scan (E_s). Finally, ΔH_e represents the decrease in conformational energy related to electrostatic repulsions between uncompensated positive charges generated on the polymer chains, which favors the opening of the polymeric structure. This term also includes an energetic component associated with mechanical stresses in the boundary between neighboring compacted and opened segments. Those repulsions and stresses act as a lever, favoring the beginning and progress of the relaxation process in order to attain a homogeneous swelling level in all the film. This extra energy can be assumed to be proportional to the anodic overpotential (η), related to an equilibrium oxidation potential (E_o) which determines the beginning of the oxidation process in open structure polymer films.[2] So the final expression for the energy required to complete 1 mol of conformational changes becomes

$$\Delta H = \Delta H^* + z_c\eta_c - z_r\eta \tag{3}$$

Parameter z_c (coefficient of cathodic polarization) can be understood as the efficiency of the electric field applied during reduction to compact the polymeric entanglement, and z_r (coefficient of electrochemical relaxation) expresses the dependence of the structure swelling on changes in the applied electric potential. Both parameters have been calculated from experimental results in a previous work.[18]

The subsequent relaxation time will be

$$\tau = \tau_o \exp\left(\frac{\Delta H^* + z_c\eta_c - z_r\eta}{RT}\right) \tag{4}$$

Equation 4 includes some approximations, the most significant of which is that every polymeric segment has the same relaxation rate (i.e. monokinetic relaxation). In fact, conformational relaxation is probably a polykinetic process, due to differences in conjugation length, film thickness, cross-linking degree, and other structural parameters between neighboring regions in the film. Our treatment will therefore be focused to on ideal case with homogeneous properties along the film. To simplify the treatment, henceforth we will make use of eq 1 instead of eq 4, but it must be noted that ΔH depends on both cathodic and anodic overpotentials.

Nucleation of Conducting Zones. The behavior described by eq 4 is valid for segments which are being relaxed in the vicinity of already relaxed segments. In those conditions, mechanical stresses and counterion concentration gradients on the boundaries between oxidized (expanded) and reduced (compacted) regions induce the creation of free volume, leading to the propagation of the conducting regions as cylinders. Nucleation at the initial stages of the oxidation, however, involves the relaxation of a first segment on the polymer/electrolyte interface, without any contact with previously relaxed zones. In those conditions, any transference of mechanical energy from relaxed to compacted segments is hindered, so the initial opening of the structure can only be influenced by the entrance of counterions from the solution and by electrostatic repulsions between charged chains. Those are electrodriven processes, so the rate of generation of oxidation nuclei will depend, similar to stress-assisted relaxation, not only on the degree of closure attained along reduction but also on the electrochemical energy given to the system along the potential scan.

To simplify the treatment, an homogeneous nucleation will be considered. Thus all the oxidation nuclei (in a number of N_o) are supposed to appear when the nucleation potential (E_N) is reached. The concomitant nucleation overpotential, defined as $\eta_N = E_N - E_o$, is related to the degree of closure of the polymeric entanglement (ϑ), expressed as the fraction of interchain free volume destroyed after polarization at a given cathodic potential E_c compared to the amount of free volume present at E_s. When $\vartheta = 0$ the structure is completely relaxed and the conformational energy required to oxidize an isolated polymeric segment is no longer the main energetic factor

affecting the oxidation rate, hence $E_N = E_o$ and $\eta_N = 0$: the potential for the beginning of the oxidation coincides with the equilibrium oxidation potential. This is a threshold state between a diffusion-controlled (open structure) and a relaxation-controlled (closed structure) oxidation process, corresponding to a cathodic potential E_s. On the other hand, when $\vartheta = 1$ the attained closure reaches its maximum value and the opening energy will be given by a saturation potential (η_N°). Assuming a linear dependence between those extreme situations, the nucleation potential can be expressed as

$$\eta_N = \eta_N^\circ \vartheta \tag{5}$$

Equation 4 will be taken as a reference in order to obtain a dependence between the degree of closure and the cathodic potential at which the polymer was reduced. The probability of occurrence of a conformational change able to allow the oxidation of an isolated segment (P) can be expressed as the inverse of the relaxation time. If all the other terms of eq 4 are included in P, then

$$P = \exp\left(-\frac{z_c}{RT}\eta_c\right) \tag{6}$$

Any increase in the cathodic potential of departure (that is, in the energy applied to the polymer during reduction) results in a decrease in the probability of a given polymer segment to undergo an opening conformational change. When $\eta_c = 0$, the structure can be considered to be open ($\vartheta = 0$) and the conformational movements required to allow the entrance of counterions within the polymer are no longer the rate controlling step, hence $P = 1$. In this case, all the segments located on the film surface can actuate as oxidation nuclei, so a planar oxidation front is formed. Contrary to this, at great values of η_c the compactness of the structure is so high ($\vartheta \approx 1$) that the probability of spontaneous conformational changes becomes very low ($P \approx 0$). Hence P is a structural parameter acting in the first moments of the oxidation process: the higher the degree of closure, the lower the probability of spontaneous conformational changes and the greater the anodic overpotential required to create a relaxation nucleus. As can be seen, this probability is directly related to the degree of closure of the polymeric entanglement. Under the hypothesis of a linear dependence between both magnitudes, we arrive at the following expression for the dependence of the degree of closure on the cathodic potential of prepolarization:

$$\vartheta = 1 - \exp\left(-\frac{z_c}{RT}\eta_c\right) \tag{7}$$

The results expressed by eqs 5 and 7 can be summarized as follows:

$$\eta_N = \eta_N^\circ\left[1 - \exp\left(-\frac{z_c}{RT}\eta_c\right)\right] \tag{8}$$

Thus, the nucleation potential will approach its maximum value asymptotically as the potential of prepolarization is shifted to more cathodic values. Equation 8 can be rearranged to obtain a linear expression:

$$\ln\left[1 - \frac{\eta_N}{\eta_N^\circ}\right] = -\frac{z_c}{RT}\eta_c \tag{9}$$

Equation 9 is suitable to be checked with experimental results, as will be seen later.

Growth of Conducting Zones. After a critically sized nucleus is formed, it starts to grow. For simplicity, it is assumed that oxidation progresses as cylinders with a base on the metal/polymer interface and the top at the polymer/electrolyte interface. After a time τ their radius increases in a length equal to λ (the length of a single polymeric segment). Under these hypotheses, the radial growth rate of each cylinder during oxidation, with v being the potential sweep rate, is given by

$$\frac{dr(\eta)}{d\eta} = \frac{\lambda}{v\tau} = \frac{\lambda}{v\tau_o}\exp[-\Delta H/RT] \tag{10}$$

This means that the rate of expansion of the oxidized regions increases during the anodic potential scan (remember eq 3), analogous to other electrochemical phase transitions reported in the literature.[44,45] This potential-dependent rate is in good agreement with experimental results from potential steps.

Integration of eq 10 yields

$$r(\eta) = \frac{\lambda}{v}\int_{\eta_N}^{\eta}\frac{d\eta'}{\tau} = \frac{RT\lambda}{z_r v\tau_o}[\exp[-\Delta H/RT] - \exp[-\Delta H_N/RT]] \tag{11}$$

where ΔH_N represents the value of ΔH at the beginning of the oxidation process (when $\eta = \eta_N$).

The effective relaxed area (once considered the overlap between neighboring expanding conductive regions) can be estimated by means of the Avrami equation.[46] Assuming the formation of N_o nucleus in the first stages of the oxidation, we arrive at

$$A(\eta) = A\left[1 - \exp\left[-\frac{\pi N_o \lambda^2}{v^2 A\tau_o^2}[RT/z_r]^2[\exp[-\Delta H/RT] - \exp[-\Delta H_N/RT]]^2\right]\right] \tag{12}$$

An expression for the faradaic charge consumed during oxidation under conformational relaxation control at each potential can be derived from eq 12, taking into account that the amount of relaxation charge consumed until a given moment is proportional to the area of the oxidized regions:

$$Q_r(\eta) = Q_r\left[1 - \exp\left[-\frac{\pi N_o \lambda^2}{v^2 A\tau_o^2}[RT/z_r]^2[\exp[-\Delta H/RT] - \exp[-\Delta H_N/RT]]^2\right]\right] \tag{13}$$

By differentiation of eq 13, an expression for the current flowing across the film along the relaxation-controlled oxidation is obtained:

$$I_r(\eta) = \frac{2\pi N_o \lambda^2}{vA\tau_o^2} Q_r \frac{RT}{z_r}\exp[-\Delta H/RT][\exp[-\Delta H/RT] - \exp[-\Delta H_N/RT]]\exp\left[-\frac{\pi N_o \lambda^2}{v^2 A\tau_o^2}[RT/z_r]^2[\exp[-\Delta H/RT] - \exp[-\Delta H_N/RT]]^2\right] \tag{14}$$

Equations 13 and 14 describe the electrochemical oxidation of a conducting polymer along an anodic potential sweep, process controlled by structural relaxation of the polymeric network and initiated through nucleation in the reduced film. They include electrochemical variables, together with structural and geometrical magnitudes related to the polymer film.

A complete quantification of the oxidation process will require diffusion equations described in next section. However, relaxation equations alone can give useful information about the evolution of the voltammetric peaks when the different electrochemical variables are changed. To derive an easily used expression from eq 14, it will be assumed that the peak overpotential (η_p) is much greater than the nucleation overpotential (η_N). In those conditions, we arrive at

$$\eta_p = \frac{\Delta H^* + z_c\eta_c}{z_r} + \frac{RT}{z_r}\ln\left[\frac{RT\lambda\nu}{z_r\,\tau_o}\sqrt{\frac{\pi N_o}{A}}\right] \qquad (15)$$

Equation 15 can be compared with experimental results shown by Figures 1−3 in a different manner for each variable in order to get a linear fit. Thus, under constant temperature and potential sweep rate, the influence of the cathodic overpotential on the peak overpotential is described by

$$\eta_p = a + b\eta_c \qquad (16)$$

Hence a linear dependence must be obtained by representing the peak potential (E_p) against the cathodic potential of departure (E_c). Upon varying the temperature, with all the other experimental parameters being kept constant, eq 15 becomes at high η_p

$$\eta_p/T = a' + b'\ln T \qquad (17)$$

A semilogarithmic representation of η_p/T against temperature must yield a linear plot. Finally, the expression corresponding to the influence of the potential scan rate on the peak overpotential is

$$\eta_p = a'' + b''\ln \upsilon \qquad (18)$$

This last dependence is of special interest, because it is one of the experimental conclusions of the pioneering work of Odin and Nechtschein[22] in the field of relaxation processes in conducting polymers. Parameters a and b can be determined if a good fit between theoretical relationships and experimental results is achieved.

Diffusion-Controlled Full Oxidation. As it has been pointed out above, once the oxidation of the polymer is initiated, another physical process coexists with the conformational relaxation-controlled expansion of conductive zones: the transport of counterions from the solution to the oxidation centers by diffusion in the solid polymer matrix. With the oxidized polymer having a conductivity of around 10^3 S cm^{-1},[47] the electric field remains constant in the film, so no migration will be present. The charge consumed under diffusion control, once the structure is relaxed, depends only on the anodic potential applied in each moment and is independent of the initial compactness of the polymer entanglement.[2] The process can be quantified using a simplified form of Fick's law

$$F(\eta) = D[\delta_{ds}(\eta) - \delta_d(\eta)]/\chi \qquad (19)$$

where $F(\eta)$ is the molar flow of counterions into the oxidized polymer; D is the diffusion coefficient (it is an almost linear function of temperature and anodic overpotential); χ is the equivalent diffusion length across the polymer whose value can be averaged to one-half of the film thickness (h), thus $\chi = h/2$; $\delta_{ds}(\eta)$ is the counterion charge density within the oxidized zones when the film attains a steady-state related oxidation to the applied potential η, and $\delta_d(\eta)$ is the real charge density stored in the conducting regions at a given potential.

We will focus our attention on an infinitesimal fraction of the polymer film formed by all the chain segments relaxed at a given anodic potential η', which can be considered as an effective potential for the beginning of the oxidation for those segments. According to eq 12, this area ($dA(\eta')$) is given by

$$dA(\eta') = \frac{A}{\nu Q_r} I_r(\eta')\,d\eta' \qquad (20)$$

where A is the overall film surface and $I_r(\eta')$ is the relaxation current flowing through the system at η' (see eq 14). Equation 19 provides a mean to calculate the diffusion charge stored in this infinitesimal portion of the polymer at a given potential $\eta > \eta'$ along the potential sweep ($dQ_d(\eta,\eta')$)

$$\frac{d[dQ_d(\eta,\eta')]}{d\eta} = \frac{2D}{h^2}[dQ_{ds}(\eta,\eta') - dQ_d(\eta,\eta')] \qquad (21)$$

where $dQ_{ds}(\eta,\eta')$ represents the steady-state diffusion charge consumed until a given potential η is reached in the considered area. Its value can be calculated by means of eq 20:

$$dQ_{ds}(\eta,\eta') = Q_{ds}(\eta)\frac{dA(\eta')}{A} \qquad (22)$$

In eq 22, $Q_{ds}(\eta)$ represents the steady-state overall charge consumed during counterion-controlled oxidation (we assume a linear dependence between $Q_{ds}(\eta)$ and η). Equations 21 and 22 can be applied to determine of the diffusion of the charge stored in this infinitesimal portion of the polymer at a potential $\eta > \eta'$ along the potential sweep:

$$dQ_d(\eta,\eta') = Q_{ds}(\eta)\frac{2\exp(-c\eta)}{\nu\eta}\frac{I_r(\eta')}{Q_r}\int_{\eta'}^{\eta} c\eta\exp(c\eta)\,d\eta \qquad (23)$$

Here, c is a potential-dependent diffusion parameter given by

$$c = \frac{D}{h^2\nu} \qquad (24)$$

Note that the diffusion coefficient is also a linear function of η. The integration of eq 23 over all the values of η' yields the diffusion charge consumed along the potential sweep in those regions where the structure was opened under conformational relaxation control:

$$Q_d(\eta) = Q_{ds}(\eta)\frac{2\exp(-c\eta)}{\nu\eta}\int_{\eta_N}^{\eta}\frac{I_r(\eta')}{Q_r}\left[\int_{\eta'}^{\eta} c\eta\exp(c\eta)\,d\eta\right]d\eta' \qquad (25)$$

The current flowing through the polypyrrole film during the diffusion-controlled oxidation can be directly obtained from eq 25:

$$I_d(\eta) = \nu\frac{dQ_d(\eta)}{d\eta} \qquad (26)$$

Thus, we arrive at

$$I_d(\eta) = \frac{2D}{h^2}\left[Q_{ds}(\eta)\frac{A(\eta)}{A} - Q_d(\eta)\right] \qquad (27)$$

Equation 27, joined with eqs 8 and 5, describes the voltammetric responses to anodic potential sweeps in conducting polymer films, with the oxidation being controlled by conformational relaxation and diffusion processes in the solid matrix. A

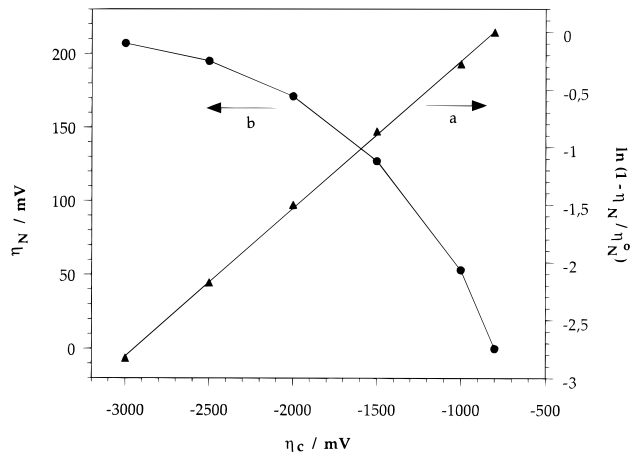

Figure 4. Plot of (a) $\ln(1 - \eta_N/\eta_N^\circ)$ vs η_c and (b) η_N vs η_c for polypyrrole films submitted to potential sweeps in the same conditions as in Figure 1, from which the nucleation parameters z_c and η_N/η_N° can be obtained.

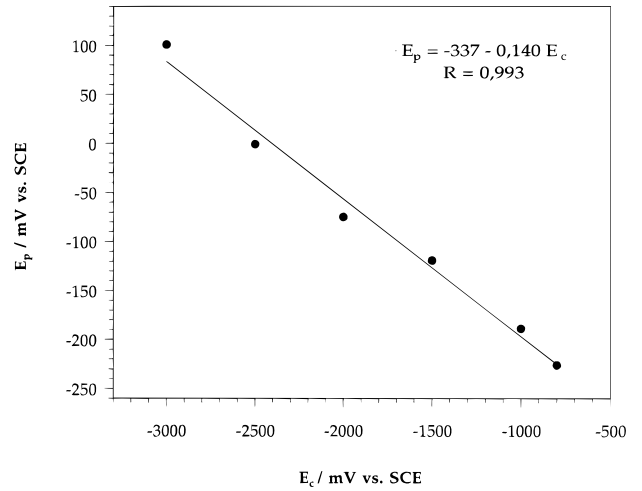

Figure 5. Evolution of the peak potential (E_p) as a function of the cathodic potential of prepolarization (E_c). Experimental data obtained from Figure 1 fit well, with eq 16.

comparison with experimental results will check the validity of the model.

5. Simulation

The validity of the developed nucleation model is confirmed by fitting eq 9 with experimental data from Figure 1: a linear shape, represented in Figure 4a, was obtained, in excellent agreement with theoretical predictions from the model. The deduced nucleation parameters are $z_c = 3192$ C mol^{-1}, which is relative to closure parameters obtained from potential steps,[18] and $\eta_N^\circ = 220$ mV, which corresponds to the extrapolated maximum value of the nucleation overpotential on Figure 4b. On the other hand, the obtained expressions for the peak potential as a function of the electrochemical variables (eqs 16−18) have been compared to experimental data from Figures 1−3, respectively. Linear fittings shown by Figure 5 for the cathodic potential, Figure 6 for the temperature, and Figure 7 for the scan rate have been obtained, as predicted by the model.

Using the above calculated nucleation parameters and the developed relaxation model (eqs 14 and 27), the experimental results depicted in Figures 1−3 have been simulated. Experimental parameters related to the polypyrrole film and required to solve those equations are: $E_o = -550$ mV,[20] $E_s = -900$ mV,[18] $N_o = 7$,[21] $\lambda/\tau_o = 4.6$ cm s^{-1} (estimated), $z_r = 3650 + 1.827(E_s - E_c)$ C mol^{-1},[18] and $z_c = 4600$ C mol^{-1}.[18] The amount of charge consumed during the overall oxidation of the

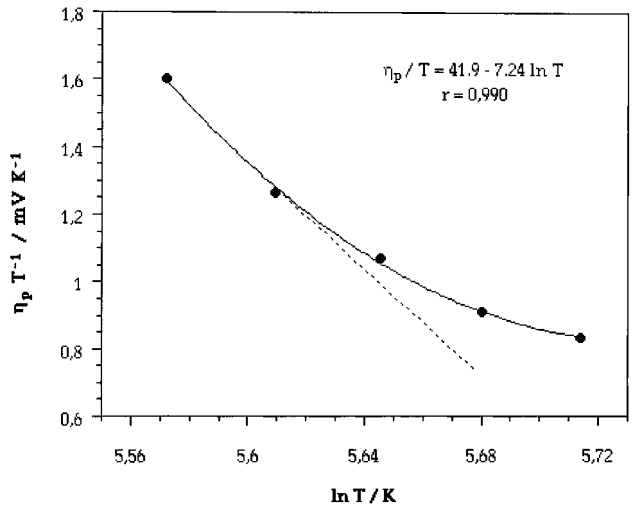

Figure 6. Plot of η_p/T vs ln T for the data extracted from Figure 2. A linear dependence was obtained, especially for low temperatures, according to eq 17.

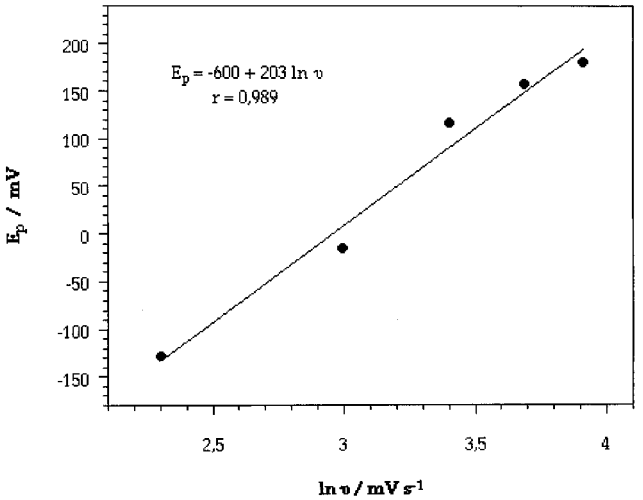

Figure 7. Semilogarithmic plot of the peak potential (E_p) vs the scan rate (υ). The linear dependence is in agreement with eq 18.

polymer in a potential sweep between −800 and 300 mV at 30 mV s^{-1} and 25 °C was 6.1 mC, according to results from Figure 1. The overall charge consumed in other experimental conditions is proportional to both the anodic overpotential applied at each moment and to the temperature, as deduced from chronoamperometry results:[18,19] $Q = 8.44 \times 10^{-5}(E - E_o)(T - T^*)$, where $T^* = -60$ °C. The fraction of charge related to the relaxation process is supposed to be a linear function of the prepolarization overpotential, being equal to $0.15Q_t$ at −3000 mV. The fitting value for ΔH is 10 kJ mol^{-1}, lower than values obtained from chronoamperometric measurements for thick films.[19] This fact is probably due to higher chain mobility in thin films. Values for the diffusion coefficient (D) can also be obtained from experimental chronoamperograms, assuming that $\delta = h/2$. Values range between 6.02×10^{-11} cm^2 s^{-1} in the reduced state ($E = -200$ mV vs SCE) and 1.05×10^{-10} cm^2 s^{-1} in the oxidized state ($E = 300$ mV). A similar variation is obtained when the temperature is changed from −10 to 40 °C. This change is caused by the opening of the polymeric structure during doping or heating.

Theoretical voltammetric responses of polypyrrole films, initiated from different cathodic potentials (ranging between −3000 and −1000 mV) up to 300 mV at 30 mV s^{-1}, are shown in Figure 8. The ESCR model is able to predict the shape of voltammograms (as did previous models in literature) as well

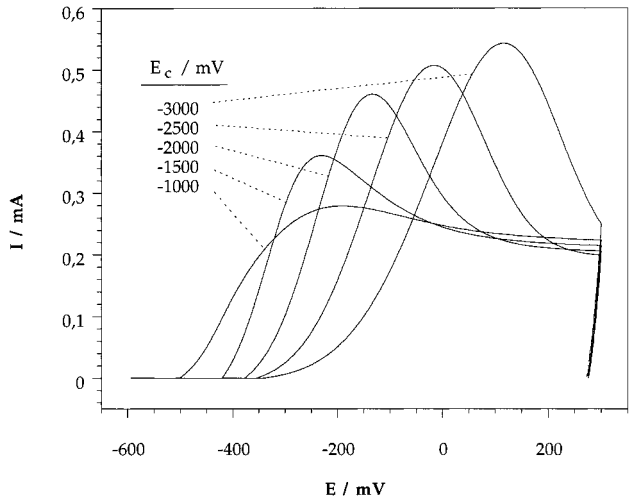

Figure 8. Theoretical simulation of a series of voltammograms, initiated from different cathodic potentials (ranging between −1000 and −3000 mV vs SCE), by application of eqs 8, 14, and 25.

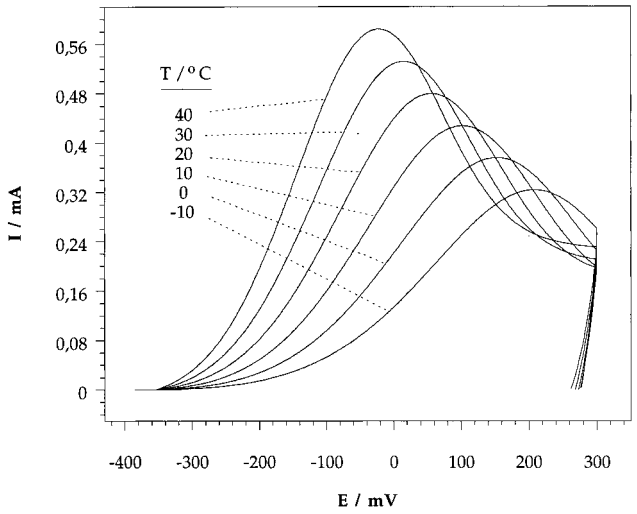

Figure 9. Theoretical simulation of voltammograms performed from −2000 to 300 mV, showing the effect of the temperature (variations indicated on the figure) on the shape of the curve and the position of the maximum.

as their evolution as a function of the cathodic potential: both nucleation potential and current peak are shifted anodically at higher cathodic prepolarization potentials, in accordance with results from Figure 1. Voltammograms simulated at different temperatures and sweep rates can be observed in Figures 9 and 10, respectively. The current peak rises and shifts, either anodically when the sweep rate increases or cathodically when the temperature rises, in accordance with experimental results. A direct comparison of theoretical and experimental potentials (E_p) and intensities (I_p) for the voltammetric current peaks is provided by Figures 11 and 12, respectively.

Current intensities associated with relaxation (eq 14) and diffusion (eq 27) processes are compared in Figure 13. Selected conditions are $E_c = -2000$ mV, $T = 25$ °C, and $v = 30$ mV s^{-1}. As can be observed, I_r (E) rises and reaches its maximum in the first moments of oxidation, when the opening of the polymeric structure is almost completed. I_d (E) rises slowly, but it defines the position of the voltammetric maximum. We conclude from these comparisons that, despite the important simplifications introduced in the model, predicted behaviors are in good agreement with experimental observations. These results suggest that the ESCR treatment is pointing in the right direction for determining structural parameters related to conducting polymers from electrochemical techniques. This should allow a complete integration of electrochemistry and polymer science, and it would mean the definitive success of the model.

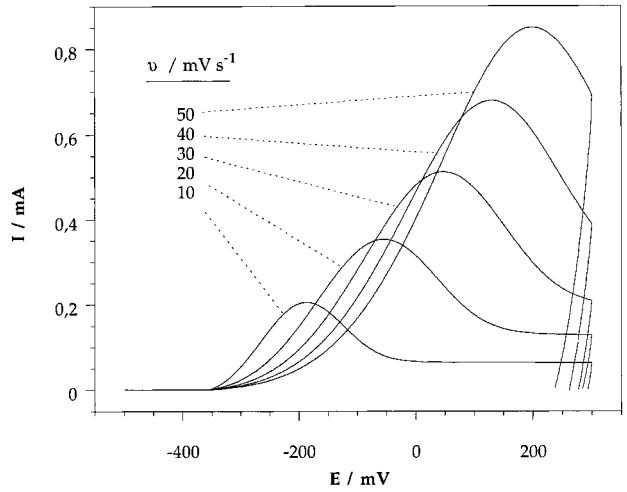

Figure 10. . Voltammetric behavior simulated for increasing scan rates (10−50 mV s^{-1}) when the cathodic potential of departure was −2000 mV, the anodic limit 300 mV, and the temperature 25 °C.

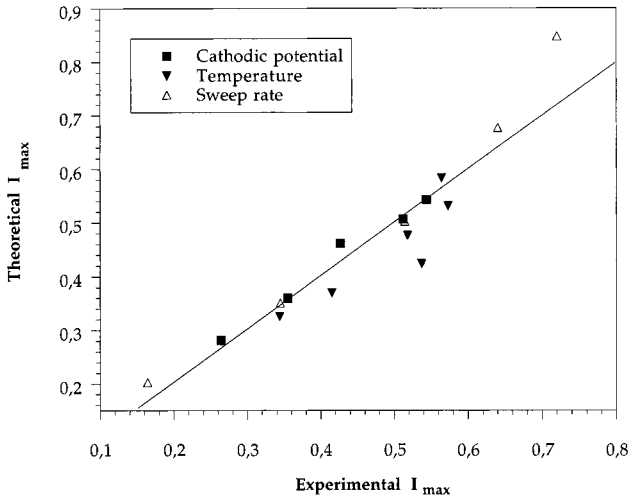

Figure 11. . Correlation between theoretical and experimental values for the current maxima (I_p) of the voltammetric curves. Data were extracted from Figures 1−3, for the cathodic potential, temperature, and sweep rate, respectively.

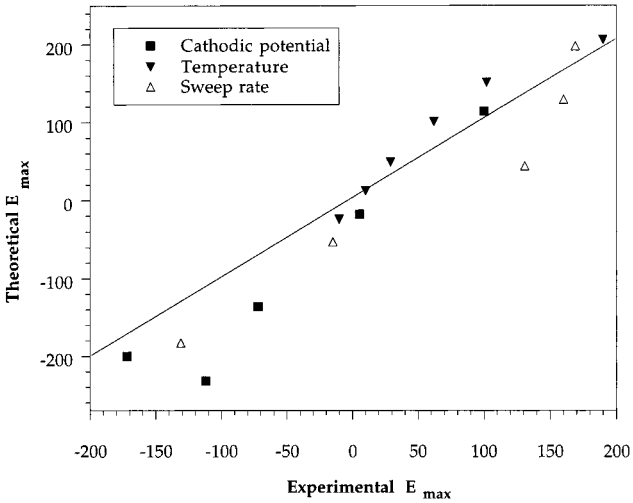

Figure 12. Correlation between theoretical and experimental values for the potentials of the current peaks (E_p) of the voltammetric curves. Data were extracted from Figures 1−3, for the cathodic potential, temperture, and sweep rate, respectively.

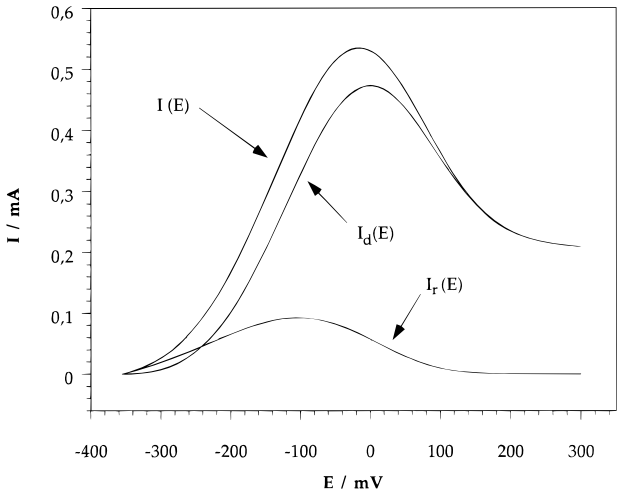

Figure 13. Separation of the overall oxidation curve into its relaxation and diffusion components according to eq 14 and 27, respectively.

6. Concluding Remarks

The objective of this paper was to develop an electrochemical theory of polymeric relaxation (rearrangement of the chain conformations accompanying the redox process) able to explain the voltammetric behavior of conducting polymers. After relaxation, other electrochemical processes are controlled and completed by diffusion. The relaxation process is quantified by a relaxation time, which depends on the anodic overpotential (oxidation level) and the cathodic overpotential (closure of the structure the neutral state). Under these conditions, and assuming nucleation-like kinetics for the advance of the oxidation front, anodic voltammograms for polypyrrole films in 0.1M $LiClO_4$/propylene carbonate solutions obtained by potential steps from different cathodic potentials at various scan rates and temperatures were simulated, fitting experimental results.

Acknowledgment. This work has been supported by the Diputación Foral de Gipuzkoa/Gipuzkoako Foru Aldundia, the Eusko Jaurlaritza/Gobierno Vasco, and the Spanish Ministerio de Educación y Cultura.

References and Notes

(1) Yeu, T.; Nguyen, T. V.; White, R. E. *J. Electrochem. Soc.* **1988**, *135*, 1971.
(2) Otero, T. F.; Angulo, E. *Solid State Ionics* **1993**, *63*−*65*, 803.
(3) Cao, J.; Aoki, K. *Electrochim. Acta* **1996**, *41*, 1787.
(4) Yap, W. T.; Durst, R. A.; Blubaugh, E. A.; Blabaugh, D. D. *J. Electroanal. Chem.* **1983**, *144*, 69.
(5) Tanguy, J.; Mermilliod, N.; Hoclet, M. *Synth. Met.* **1987**, *18*, 7.
(6) Tezuka, Y.; Aoki, K. *J. Electroanal. Chem.* **1989**, *273*, 161.
(7) Kaplin, D. A. ; Qutubuddin, S. *J. Electrochem. Soc.* **1993**, *140*, 3185.
(8) Yeu, T.; White, R. E. *J. Electrochem. Soc.* **1990**, *137*, 1327.
(9) Heinze, J.; Bilger, R. *Ber. Bunsen-Ges. Phys. Chem.* **1993**, *97*, 502.
(10) Posey, F. A.; Morozumi, T. *J. Electrochem. Soc.* **1966**, *113*, 176.
(11) Vorotyntsev, M. A.; Vieil, E.; Heinze, J. *Electrochim. Acta*, **1996**, *41*, 1913.
(12) Feldberg, S. W. *J. Am. Chem. Soc.* **1984**, *106*, 4671.
(13) Doherty, T.; Sunderland, J. G.; Roberts, E. P. L.; Pickett, D. J. *Electrochim. Acta* **1996**, *41*, 519.
(14) Hillman, A. R.; Bruckenstein, S. *J. Chem. Soc., Faraday. Trans.* **1993**, *89*, 339.
(15) Kok, W. T.; Tüdös, A. J.; Poppe, H. *Analytica Chimica Acta* **1990**, *228*, 39.
(16) Aoki, K.; Tezuka, Y. *J. Electroanal. Chem.* **1989**, *267*, 55.
(17) Albery, W. J.; Mount, A. R. *J. Electroanal. Chem.* **1995**, *388*, 1.
(18) Otero, T. F.; Grande, H.; Rodríguez, J. *J. Electroanal. Chem.* **1995**, *394*, 211.
(19) Otero, T. F.; Grande, H. *J. Electroanal. Chem.* **1996**, *414*, 171.
(20) Otero, T. F.; Grande, H.; Rodríguez, J. *Synth. Met.* **1996**, *76*, 293.
(21) Otero, T. F.; Grande, H.; Rodríguez, J. *J. Phys. Chem. B* **1997**, *101*, 3688.
(22) Odin, C.; Nechtschein, M. *Synth. Met.* **1993**, *55*−*57*, 1281.
(23) Chiarelli, P.; De Rossi, D.; Della Santa, A.; Mazzoldi, A. *Polym. Gels Networks* **1994**, *2*, 289.
(24) Otero, T. F.; Angulo, E.; Rodríguez, J.; Santamaría, C. *J. Electroanal. Chem* **1992**, *341*, 369.
(25) Otero, T. F.; Sansiñena, J. M. *Bioelectrochemis. Bioenerg.* **1995**, *38*, 411.
(26) Otero, T. F.; Rodríguez, J.; Angulo, E.; Santamaría, C. *Synth. Met.* **1993**, *55*−*57*, 3713.
(27) Tsai, E. W.; Pajkossy, T.; Rajeshwar, K.; Reynolds, J. R. *J. Phys. Chem.* **1988**, *92*, 3560.
(28) Zhou, D.; Zhao, H.; Price, W. E.; Wallace, G. G. *J. Membr. Sci.* **1995**, *98*, 173.
(29) Ehrenbeck, C.; Jüttner, K. *Electrochim. Acta* **1996**, *41*, 511.
(30) Wang, E.; Liu, Y.; Dong, S.; Ding, J. *J. Chem. Soc., Faraday Trans.* **1990**, *86*, 2243.
(31) Marque, P.; Roncali, J. *J. Phys. Chem.* **1990**, *94*, 8614.
(32) Qiu, Y.; Reynolds, J. R. *Polym. Eng. Sci.* **1991**, *31*, 6.
(33) Heinze, J.; Störzbach, M.; Mortensen, J. *Ber. Bunsen-Ges. Phys. Chem.* **1987**, *91*, 960.
(34) Otero, T. F.; Grande, H. *Colloids Surf., A*, in press.
(35) Teorell, T. *Trans. Faraday Soc.* **1937**, *33*, 1054.
(36) Meares, D.; Thain, J. F.; Dawson, D. G. In *Membranes*; Eiseman, G., Ed.; Marcel Dekker: New York, 1972; Vol. 1.
(37) Odin, C.; Nechtschein, M. *Phys. Rev. Lett.* **1991**, *67*, 1114.
(38) Odin, C.; Nechtschein, M. *Synth. Met.* **1993**, *55*−*57*, 1287.
(39) Villeret, B.; Nechtschein, M. *Phys. Rev. Lett.* **1989**, *63*, 1285.
(40) Inzelt, G.; Horányi, G.; Chambers, J. Q. *Electrochim. Acta* **1987**, *32*, 757.
(41) Inzelt, G.; Day, R. W.; Kinstle, J. F.; Chambers, J. Q. *J. Phys. Chem.* **1983**, *87*, 4592.
(42) Aoki, K.; Cao, J.; Hoshino, Y. *Electrochim. Acta* **1994**, *39*, 2291.
(43) La Croix, J.; Díaz, A. F. *Makromol. Chem., Macromol. Symp.* **1987**, *8*, 17.
(44) *Instrumental methods in electrochemistry*; Southampton Electrochemistry Group; John Wiley & Sons: New York, 1985.
(45) Sánchez Maestre, M.; Rodríguez-Amaro, R.; Muñoz, E.; Ruiz, J. J.; Camacho, L. *J. Electroanal. Chem.* **1994**, *373*, 31.
(46) Avrami, M. *J. Chem. Phys.* **1939**, *7*, 1103; **1940**, *8*, 212; **1941**, *9*, 177.
(47) Diaz, A. F.; Castillo, J. I.; Logan, J. A.; Lee, W. Y. *J. Electroanal. Chem.* **1981**, *129*, 115.